

RED-ACT Report

Real-time Earthquake Damage Assessment using City-scale Time-history analysis

Mar. 16, M7.4 Fukushima Coast, Japan Earthquake

Research group of Xinzheng Lu at Tsinghua University (luxz@tsinghua.edu.cn)

First reported at 23:11, Mar. 16, 2022 (Beijing Time, UTC +8)

Acknowledgments and Disclaimer

The authors are grateful for the data provided by **K-NET** and **KiK-net**. This analysis is for research only. The actual earthquake damage should be determined according to the site investigation.

Scientific background of this report can be found at: <http://www.luxinzheng.net/rr.htm>

1. Introduction to the earthquake event

At 23:36 Mar. 16 2022 (Local Time, UTC +9), an **M 7.3** earthquake occurred in **Fukushima Coast, Japan**. The epicenter was located at **141.95 37.65**, with a depth of **60 km**.

2. Recorded ground motions

31 ground motions near to epicenter of this earthquake were analyzed. The names and locations of the stations can be found Table 1. The typical recorded peak ground acceleration (PGA) is **745** cm/s/s. The waveform and corresponding response spectra in comparison with the design spectra specified in the Chinese Code for Seismic Design of Buildings are shown in Figure 1.

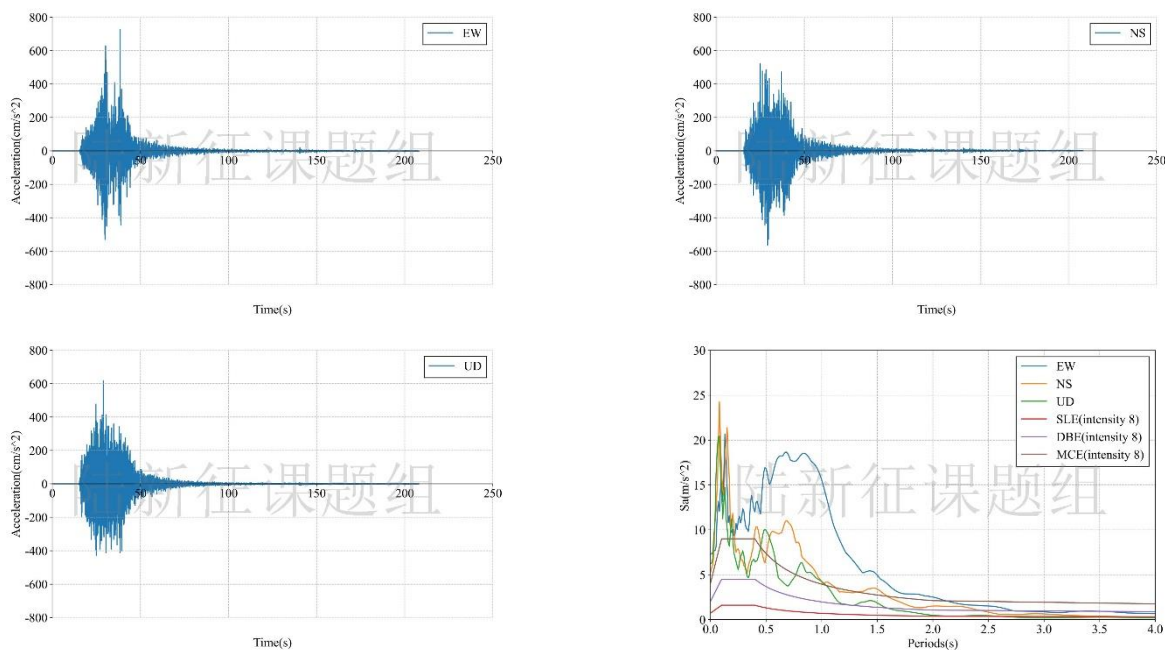


Figure 1 Waveform and response spectra of the recorded ground motions with maximal PGA

3. Damage analysis of the target region subjected to the recorded ground motions

Using the real-time ground motions obtained from the strong motion networks and the **city-scale nonlinear time-history analysis**, the damage ratios of buildings located in different places can be obtained. The building damage distribution and the human feeling distribution near to different stations are shown in Figure 2 and Figure 3, respectively. These outcomes can provide a reference for post-earthquake rescue work. Note that during the 2011 Tohoku earthquake, the buildings in the Fukushima region have already experienced strong shaking. Consequently, the seismic resistance of the buildings should be stronger than the average level.

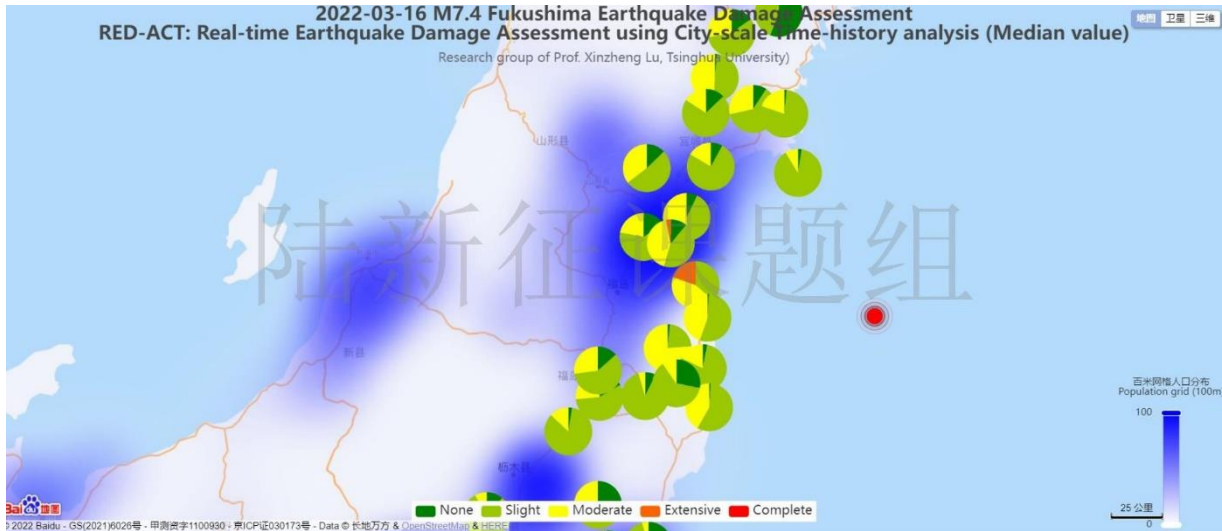


Figure 2 Damage ratio distribution of the buildings near to different stations

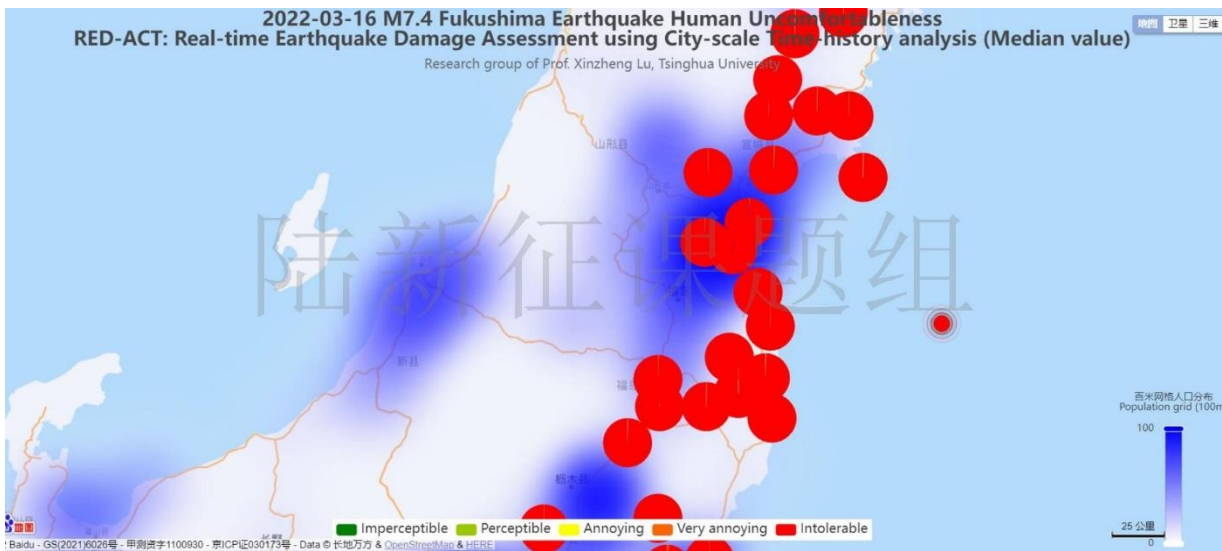
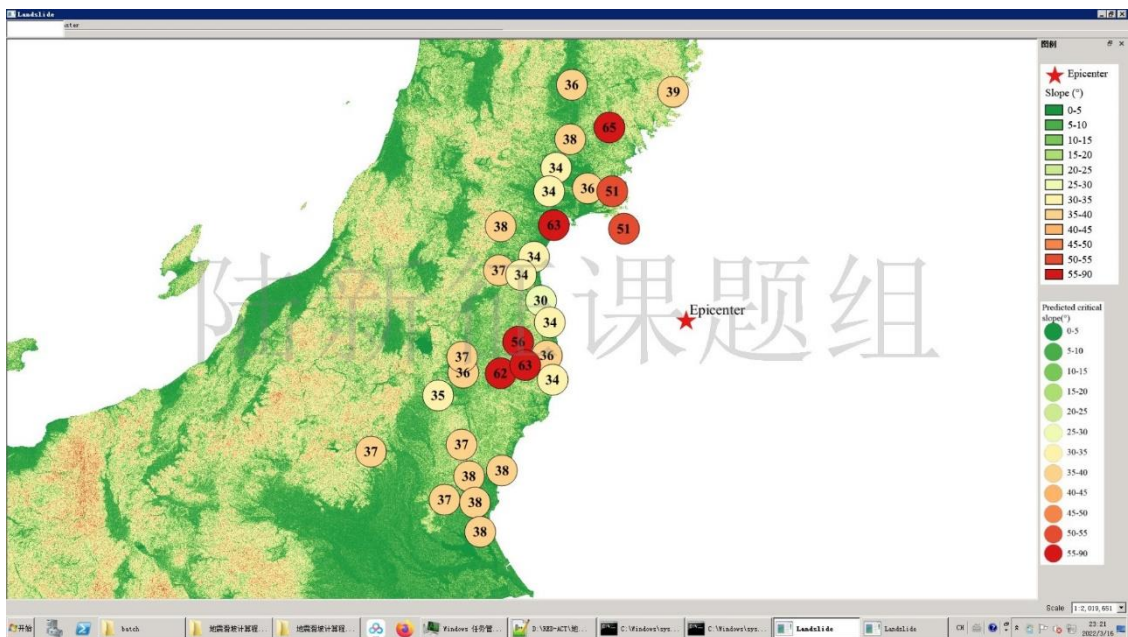


Figure 3 Human feeling distribution near to different stations

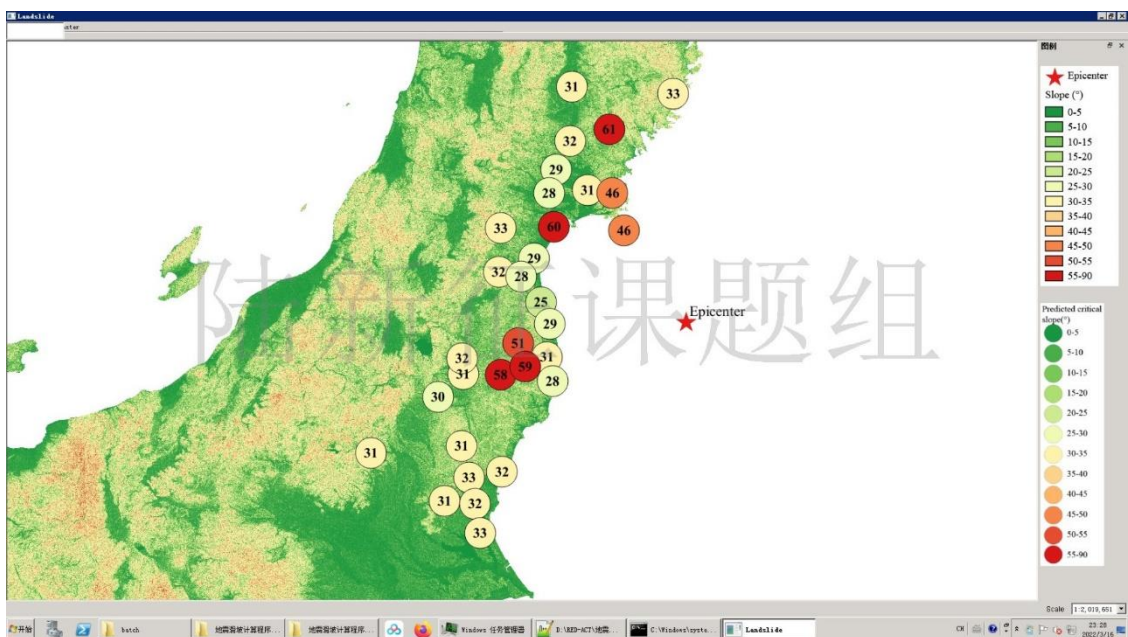
4. Earthquake-induced landslide of the target region subjected to the recorded ground motions

According to local topographic data, lithology data and ground motion records, the distribution of earthquake-induced landslide near to different stations under the different proportions of the landslide slab thickness that is saturated can be calculated, as shown in Figure 4. The basemap shows the distribution of the local

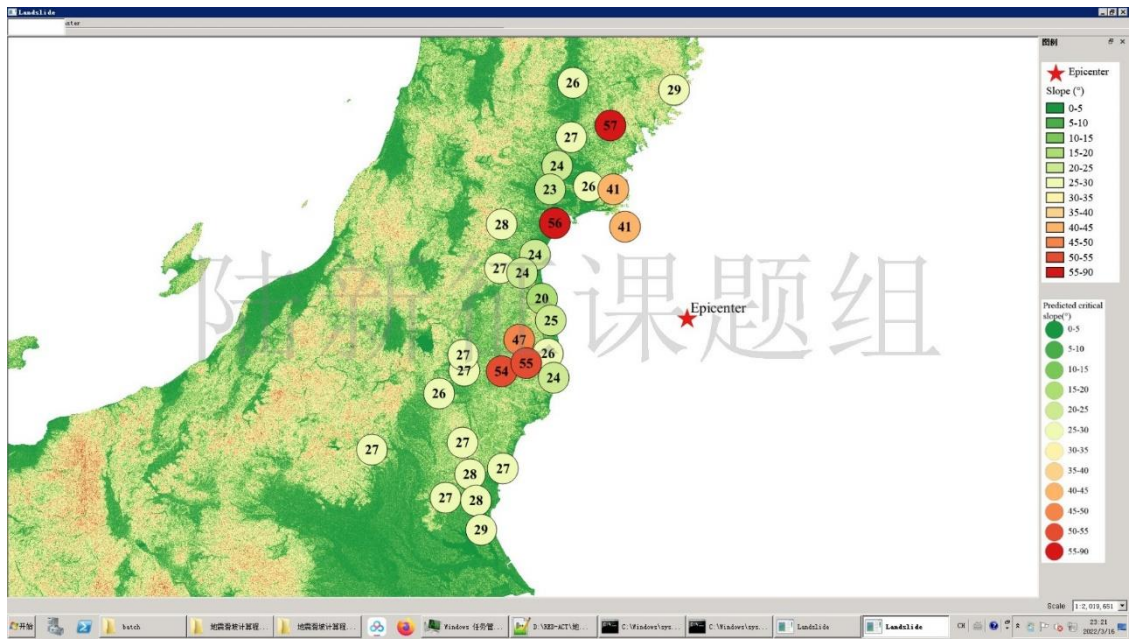
slope. The number in the circle represents the critical slope of the landslide. The earthquake-induced landslide tends to occur with a higher probability when the slope is larger than this threshold value.



(a) The proportion of the landslide slab thickness that is saturated equals 0%



(b) The proportion of the landslide slab thickness that is saturated equals 50%



(c) The proportion of the landslide slab thickness that is saturated equals 90%
 Figure 4 Distribution of earthquake-induced landslide near to different stations

Scientific background of this report can be found at: <http://www.luxinzheng.net/rr.htm>